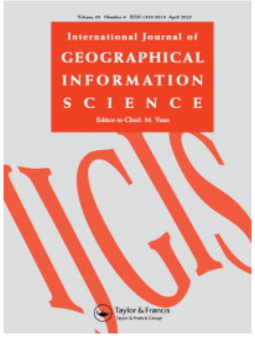

Taylor & Francis
Taylor & Francis Group

International Journal of Geographical Information Science

ISSN: (Print) (Online) Journal homepage: www.tandfonline.com/journals/tgis20

Disaster vulnerability in road networks: a data-driven approach through analyzing network topology and movement activity

Danial Alizadeh & Somayeh Dodge

INTERNATIONAL JOURNAL OF GEOGRAPHICAL INFORMATION SCIENCE
https://doi.org/10.1080/13658816.2024.2411001

RESEARCH ARTICLE

OPEN ACCESS

Disaster vulnerability in road networks: a data-driven approach through analyzing network topology and movement activity

Danial Alizadeh and Somayeh Dodge

Department of Geography, University of California Santa Barbara, Santa Barbara, CA, USA

ABSTRACT

The rise in natural disasters and climate-induced events, such as wildfires, hurricanes, and flooding, has significantly affected urban life. These events can disrupt daily activity and flows of individuals and goods on road and transit networks. To enhance urban resilience against disasters, it's crucial to study and understand road network vulnerability, utilizing data-driven insights to inform planning and preparedness efforts. The aim of this paper is to develop a data-driven exploratory approach to assess vulnerability in road networks in response to a disruption. To accomplish this, we compare the centrality of road segments before, during, and after disaster, considering the network topological structure and movement activity as it is observed through large tracking data of cellphone traces on the network. The novelty of our approach lies in inferring the impact from movement data, instead of manually removing links from the network. The results obtained from this study suggest that incorporating movement data into the assessment of network functionality provides a more realistic estimation of the road network vulnerability in response to a disruption, compared to solely using network topology.

ARTICLE HISTORY
Received 7 March 2024
Accepted 25 September 2024

KEYWORDS
Data-driven movement analysis; network centrality; road network vulnerability; urban resiliency; complex network theory

1. Introduction

The vulnerability of road networks to disruptions has been a significant concern in resilience research (Matisziw and Murray 2009, Furno *et al.* 2021). Various events, such as natural disasters, accidents, or infrastructure failures, can lead to disruptions that impact people's daily lives and access to essential services. For instance, major wildfires can significantly disrupt road travel for several weeks by prompting safety closures or causing traffic congestion due to widespread evacuations (Fraser *et al.* 2022). Urban resiliency is tightly associated with road network vulnerability (Mattsson and Jenelius 2015). That is, when an important road network becomes disabled, the overall

CONTACT Danial Alizadeh danial_alizadeh@ucsb.edu

functionality of a city can be greatly affected. Therefore, studying and understanding the vulnerability of road networks to disasters is crucial, and can provide valuable insights for policymakers to enhance urban resilience.

In transportation engineering, a road network is modeled as a graph consisting of a set of nodes and links representing intersections and road segments, respectively (Jayasinghe *et al.* 2019). The concept of road network vulnerability is defined as the network susceptibility against disruptions that can lead to a reduction in network performance or serviceability (Sun *et al.* 2015, Huang and Loo 2023). Disruptions threatening road networks can be generally divided into two categories, including natural disasters (e.g. wildfires, floods, earthquakes) and human-induced disruptions (e.g. terrorist attacks, infrastructure failure, traffic crashes) (Testa *et al.* 2015, Huang and Loo 2023). Depending on the severity and proximity of a disruption, a single or several road network elements (e.g. intersections or road segments) may lose their functionality, causing a change in the road network topology and connectivity. As such, one reasonable way to quantify the road network vulnerability is to measure the extent to which the network topology changes due to a disruption. However, topology alone cannot inform us about how movement patterns are impacted on the network in response to the disruption.

Centrality measures, including *node degree*, *closeness*, and *betweenness* are commonly used to quantify network topology. Originating from graph theory, network analysis and centrality measures (Freeman *et al.* 2002) have been applied in many fields, such as sociology, biology, computer science, transportation, and communication to assess connectivity and access (Zhang *et al.* 2011). These measures can be used as indicators to assess the importance or prominence of network elements (e.g. nodes) with respect to certain criteria. For instance, degree centrality counts the number of connections a node has with its neighboring nodes. A node with a higher degree is regarded as more prominent or important, as it's connected to many other nodes in the network. Closeness centrality, on the other hand, measures how close a node is to the other nodes. While betweenness centrality counts the number of times a node is located on the shortest paths between any pairs of nodes in the network (Shi *et al.* 2019). Among centrality measures, betweenness is recognized as the most effective measure in capturing the vulnerability of the road segments (Ahmadzai *et al.* 2019). That is, a road segment is considered to be vulnerable if that segment lies on many shortest paths. As a result, removal of such road segment affects the connectivity between many nodes, which ultimately disrupts movement on a larger part of the network and creates longer detours (Demšar *et al.* 2008). Considering the importance of vulnerable road segments, they can be highly susceptible to disruptive events (Furno *et al.* 2021). Therefore, to ensure road network functionality during disruptions, it is crucial to proactively identify vulnerable road segments and implement measures to safeguard them against disruptions.

In this study, we use betweenness to examine the vulnerability of road networks before and after a disruption occurs. In addition to the spatial structure of the roads and network topology, we take account of the real movement patterns on the road network as observed through cellphone tracking data. We apply this approach to analyze road network vulnerability during a wildfire event in California, assessing how well the developed methodology can capture the impact of such events on transportation systems. This paper extends the existing literature by integrating both network topology and movement patterns to assess the road network vulnerability.

The remainder of this article is structured as follows. Section 2 provides an overview of previous work in this area. Section 3 describes the proposed methodology. Sections 4 and 5 present and discuss the results through a case study, and finally, Section 6 summarizes the findings of this paper.

2. Background

Murray *et al.* (2008) categorize approaches that are used to assess the vulnerability of networks to random and intentional disruptions into four groups: scenario-specific, strategy-specific, simulation, and mathematical models. Scenario-specific approaches examine how network efficiency might be impacted if, for example, one or several network elements (e.g. nodes or edges) become disabled due to a disruption (Suarez *et al.* 2005). In contrast, strategy-specific models are used to assess network vulnerability against a series of coordinated disruption (e.g. terrorist attacks). In these models, network elements are commonly ranked based on their importance, and then removed successively. Subsequently, network efficiency is evaluated after the removal of each element (Albert *et al.* 2000). The relative importance of network elements are usually obtained from topological analysis of the road networks. There exist many feasible scenarios in which the network might be impacted. Considering all the possible scenarios is computationally intense, especially when the network is structurally complex or large. Simulation models, however, are used to measure the impacts of only a range of possible scenarios on the network vulnerability. For instance, in the research conducted by Matisziw *et al.* (2009), a specific number of nodes are removed from the network in each scenario. Subsequently, Origin-Destination (OD) path availability along with network flow are computed to measure network vulnerability caused by each scenario. Mathematical models are utilized to identify the scenarios in which the network is impacted the most (Church *et al.* 2004), for example, using flow optimization (Matisziw and Murray 2009). In their work, a path is available between two nodes only if they are physically connected over the network. However, in reality, the availability of a path may also depend on several attributes of road segments, including available capacity, traffic volume, transportation cost, and road type. For example, while a path may appear physically feasible between two nodes (e.g. two intersections), it could surpass its capacity threshold due to high traffic volume, thereby making the nodes inaccessible. Therefore, it is vital to develop new models capable of incorporating road segment attributes along with network topology. In this regard, there are few studies focusing on integrating movement data (e.g. traffic volume, density of vehicles on each road segment), with network topology to strengthen their model. For example, Sun *et al.* (2015) take into account not only the network topology but also the passenger flow to measure the vulnerability of Shanghai rail transit network. In their study, network efficiency, defined as the sum of the inverse values of the shortest paths between each pair of nodes, is utilized as a measure of network vulnerability. Huang and Loo (2023) incorporate speed as an example of road attributes into their model. They defined an index called congestion index (CI), taking both the actual speed and the speed limit on each road segment into account. There is another avenue of research in which the vulnerability of a road network is quantified using accessibility measures. For instance, Papilloud and Keiler (2021) developed two modified gravity-based accessibility measures to quantify the vulnerability changes caused by a flood. Their modified accessibility index is a function of 'populations impacted by the flood', 'opportunities' (e.g. the total number of employment places and schools) in each traffic zone, and the 'average shortest travel time'. Their findings indicate that different spatial scales (e.g. the entire study area or traffic zone) produce different vulnerability results. As a measure of vulnerability, Taylor (2008) computes variations in accessibility caused by a disruption through subtracting the pre-disruption accessibility values from the post-disruption accessibility values. The index utilized in their study calculates the accessibility of an individual to an activity rather than the accessibility between different locations. Gu *et al.* (2022) also introduce a utility-based accessibility metric to evaluate the vulnerability of a multi-modal transportation network (e.g. cars, buses, and metros). Their findings suggest that utility-based accessibility metrics outperforms other models in assessing vulnerability, as they can incorporate travel choice behavior effectively.

Topology-based network vulnerability assessment approaches often utilize different measures. For example, Sun *et al.* (2018) employ several well-known topology metrics, such as node degree, betweenness, and the strength to examine the susceptibility of the rail transit network. Testa *et al.* (2015) utilize several other topological metrics, including average nodal degree, and clustering coefficient to measure the vulnerability of the coastal transportation networks against extreme climate events. In their study, nodes and links are randomly eliminated to simulate the impact of extreme weather, and model the impacted network. These metrics are then computed on both original and impacted network to compare and evaluate network vulnerability. In most of existing studies, to re-construct the impacted network after the disruption, nodes or links (e.g. intersections or road segments) of the network are eliminated from the network either randomly or intentionally. In the random approach, a certain number of nodes/links are removed randomly from the network to obtain the impacted network. In the intentional removal approach, the most important links (e.g. the links with the highest value of betweenness/degree) are removed from the network. These approaches often assess vulnerability based on hypothetical scenarios (e.g. potential closures due to flooding). Comparing both approaches, Shi *et al.* (2019) demonstrate that the network can be more susceptible to intentional than random removal of links. Their findings suggest that random removal of the links may not be an effective approach in assessing network vulnerability, where the goal is to identify the worst-case scenarios. Boeing and Ha (2024) measure the vulnerability of road networks across different urban areas in the world to various types of disruptions (e.g. intentional and random disruptions). In their study, road network vulnerability is computed based on two indices, *robustness* and *efficiency*. Robustness is defined as the proportion of OD pairs that persist following each disruption to the network, while efficiency refers to the average inverse of the shortest path distance among all OD pairs after the disruption. Their results suggest that networks with higher connectivity, fewer chokepoints, or less circuity are less vulnerable to disruptions. Such approaches could be strengthened by incorporating insights from real movement patterns during disruptions. This helps to gain a more holistic estimation of the road network vulnerability. In this paper, we aim to advance road network vulnerability analysis through a scenario-specific, and data-driven approach that considers both network topology and movement activity on the road network before and after a disruption.

3. Methodology

Our proposed data-driven methodology relies on anonymized, opted-in observed GPS traces from cellphones and other location aware technologies (LATs) such as smartwatches, wearable fitness trackers, tablets, etc. These data, which are often acquired from location intelligence companies (e.g. Spectus, Veraset), are used as an indicator of movement activity over the road network, helping to assess changes in road usage before and after the occurrence of a disruptive event (e.g. wildfire, hurricane, car crash). Using such large and high resolution GPS tracking data, the methodology consists of three main processes: First, movement trajectories are pre-processed (e.g. through filtering and outlier detection) and assigned to road segments via a map matching process to quantify the number of vehicles at each road segment and over time. Second, variations in movement activity and potential road closures in response to a disruption are quantified from movement data, considering both speed and vehicle counts on roads. Third, the vulnerability across the impacted road network is analyzed and compared using both network topology and movement activity information. And finally, a difference map is created to highlight the disparities between outcomes derived solely from network topology and those incorporating both network topology and movement data. Figure 1 summarizes the methodology used in this study. Each step is described in detail below.

3.1. Map matching

Map matching is a prerequisite process to connect raw trajectory data to the right road segments and quantify activity (i.e. trajectory counts) on each road segment. There are many approaches to map matching: For examples, Quddus *et al*. (2007) compare different map matching techniques, such as point-to-point matching, point-to-curve matching, and probabilistic models. Similarly, Chao *et al*. (2020) perform several map matching models to assess the varying effects of different models on the map matching outcomes. These comparative analyses suggest that the majority of the existing map matching models are time-intensive and error-prune, especially when applied to high-frequency and large data sets (Zhu *et al*. 2022).

In this study, to perform map matching, we consider a commonly-used approach incorporating a spatial buffer around each road segment. The number of trajectories intersecting each road segment buffer on a given day is then assigned to the respective road segment. To speed up the computation, we employ spatial indexing, which helps to efficiently identify candidate geometries that may satisfy the spatial

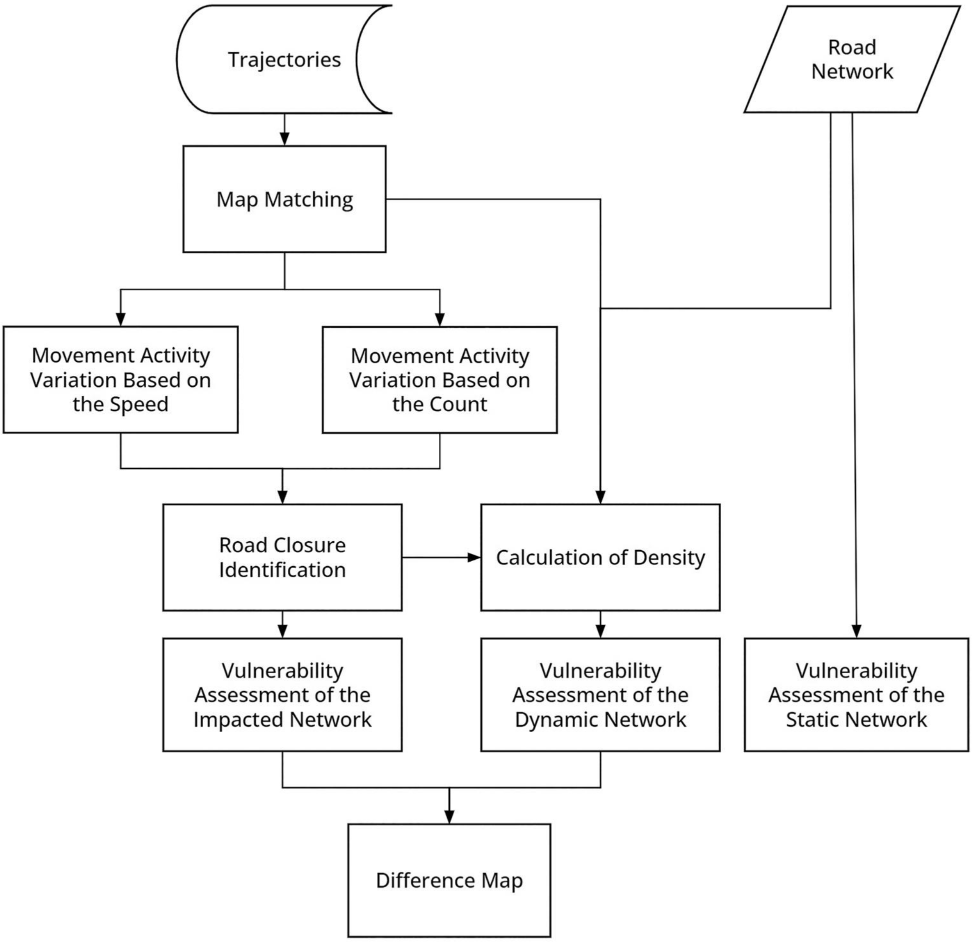

Figure 1. An overview of the methodological workflow.

relationship (e.g. intersect, contain, and overlap) being queried (Boeing 2016). That is, it reduces the number of geometries that need to be examined for the operation, thus speeding up the computation. On the other hand, the state-of-the-art map matching models, such as deep-learning models (Feng *et al.* 2020), mainly require to be trained first on a relatively large amount of data, leading to a more computationally expensive process (Hu and Lu 2019). It is worth mentioning that any other map matching technique can also be incorporated into this step.

3.2. Movement activity variation

To assess changes in movement activity in response to a disruption, it's essential to establish a baseline from which variations are computed. To measure daily variation in movement activity on a given road segment, we first define a baseline (as described later) for each road segment, and then calculate variations from that baseline. The amount of variation from the baseline is then used to infer non-functional road segments or segments that are heavily impacted during or after the disruption. To quantify variations in movement activity, we introduce two indices based on trajectory counts and speed, as described in Sections 3.2.1 and 3.2.2.

3.2.1. Quantifying movement activity variation based on trajectory counts

To assess variations in movement activity in terms of road usage, we compute the baseline for each road segment (TC_i for the ith road segment) by deriving the median trajectory count recorded for that segment across the entire study period (e.g. n days), using Equation (1). The rationale for selecting the median over other measures, such as the mean, is that it is more robust against outliers (Moore and McCabe 1989). The daily variation in movement activity for each road segment i is then calculated as the ratio of the daily trajectory count ($TC_{(i,t_j)}$, $1 \le j \le n$ days) divided by the baseline (Equation 2). In this index, a value of one signifies no deviation from the baseline on a specific road segment on the respective day. A value >1 indicates an increase in trajectory counts compared to the baseline, whereas a value <1 suggests a decrease in movement activity along the segment.

$$TC_i = Median(TC_{i,t_1}, TC_{i,t_2}, TC_{i,t_3}, \ldots, TC_{i,t_n}) \tag{1}$$

Where, TC_i represents the median of trajectory counts for the road segment i during the study period, and TC_{i,t_j} denotes the trajectory count on the road segment i on day $t_j \in [t_1, t_n]$ (i.e. the jth day of the study period).

$$MV_{TC(i,t_j)} = \frac{TC_{(i,t_j)}}{TC_i} \tag{2}$$

Where, $MV_{TC(i,t_j)}$ is movement variation based on trajectory counts on the road segment i on day $t_j \in [t_1, t_n]$.

3.2.2. Quantifying movement activity variation based on speed

To assess the variation of speed on the road network, we consider the median speed of trajectories on a specific road segment i during the study period ($[t_1, t_n]$) as the speed baseline for that segment (e.g. S_i in Equation 3). Subsequently, speed variations ($MV_{S(i,t_j)}$), for the road segment i, at time t_j, is computed using Equation (4).

$$S_i = Median(S_{i,t_1}, S_{i,t_2}, S_{i,t_3}, \ldots, S_{i,t_n}) \tag{3}$$

Where, S_i is the speed baseline for segment i, and $t_j \in [t_1, t_n]$ is the jth day during the study period.

$$MV_{S(i,t_j)} = \frac{S_{(i,t_n)}}{S_i} \tag{4}$$

Where, $MV_{S(i,t_j)}$ is the movement variation based on the observed speed on the road segment i on day $t_j \in [t_1, t_n]$.

3.2.3. Road closure identification

Using movement trajectory data, road segments that become non-functional due to the disruption are identified. To do so, we performed Inter-Quartile Range (IQR) (Tukey *et al.* 1977) on the movement activity variations based on counts and speed for each road segment during our study period. A road segment is identified as non-functional on a certain day if both the corresponding movement activity variations based on count and speed fall below the lower bound of the box plot (i.e. $Q1-(1.5\times IQR)$, where $Q1$ is the value of the first quantile). We incorporate both speed and counts in the identification of road closures because a road segment might have a trajectory speed below the lower bound of the box plot, while still having trajectory counts above the lower bound. This case could indicate traffic congestion rather than road closures. Thus, considering solely either counts or speeds is inadequate in identifying road closures.

3.3. Vulnerability assessment

3.3.1. Vulnerability assessment of the static network

The spatial structure or topology of a road network can be modeled as a static graph consisting of nodes and edges. In this context, 'static' denotes that the network's topology remains fixed over time unless a road segment is physically removed. Equation (5) quantifies Betweenness Centrality (BC) calculated for edges following Brandes (2001, 2008), as a key indicator of vulnerability within such static network. In this study, we use the *edge betweenness centrality* function implemented in the NetworkX Python package (Hagberg *et al.* 2008) to compute the betweenness values for edges.

$$BC_k=\sum_{i,j\in V}\frac{ShortestPath_k(i,j)}{ShortestPath(i,j)} \tag{5}$$

Where, for a network of size N nodes, BC_k denotes the betweenness value for the edge k, $ShortestPath_k(i,j)$ $(i,j\in[1,N])$ represents the number of shortest paths between node i and j passing through edge k, and $ShortestPath(i,j)$ stands for the total number of shortest paths between nodes i and j.

A greater value of BC_k indicates that edge k is more frequently positioned along the shortest paths within the network, highlighting its higher importance in network connectivity. Consequently, any impact on this edge could significantly disrupt the accessibility to various network locations and increase the network's vulnerability.

To assess changes in the vulnerability in an impacted network in response to a disruption, we first identify non-functional roads using movement data, as described in Section 3.2, and then eliminate them from the network. The network that is created after removing non-functional road segments is called the *impacted network*. We then calculate BC over the impacted network, representing the vulnerability of the static network after the impact.

3.3.2. Vulnerability assessment of the dynamic network

Vulnerability assessment of the impacted network can measure road network vulnerability based only on the network topology (e.g. the vulnerability of the static network after the impact). This, however, does not include the actual network usage, and therefore, it cannot be a holistic estimation of network vulnerability. To improve this, the vulnerability assessment is performed on a 'dynamic network' that is created by annotating each road segment with the daily density of activity, as formalized in

Equation (6).

$$Density_{(i,t_j)} = \frac{trajs(i,t_j)}{l_{(i)}} \tag{6}$$

Where, $Density_{(i,t_j)}$ represents the density on the road segment i at the time interval t_j, $trajs_{(i,t_j)}$ is the number of trajectories on the road segment i at the time interval of t_j, and $l_{(i)}$ denotes the length of the segment i. $t_j \in [t_1, t_n]$ is, for example, a day in the study period.

Shortest paths within a network can be obtained with respect to different costs (e.g. travel time, travel distance, etc.). For example, when cost is set to represent time, the shortest path between nodes a and b seeks to minimize the travel time from a to b. In the calculation of *BC* for the dynamic network, the cost of each road segment is set as the inverse of the density value obtained from the number of cellphone trajectories observed on that road segment. The *BC* values derived from the dynamic road network are then referred to as the *vulnerability of the dynamic network*.

3.4. Mapping changes in road network vulnerability and utilization

In the last step, we create a difference map to assess the impact of the disruption on the road network vulnerability. The *BC* derived from the impacted network gives an estimation of vulnerability based on network topology and road closures. The *BC* obtained from the dynamic network reflects a more holistic estimation of changes in vulnerability based on the observed movement patterns as experienced on the road before, during, and after the disruption. To differentiate the vulnerability values from the static network and the dynamic network, a difference map is created. In this map, the value represented on each road segment is obtained by subtracting the vulnerability values of the static network from those of the dynamic network. As a result, a value of 0 represents no change, while a positive value represents over-utilization of those road segments compared to what is expected. A negative value indicates an under-utilization of the road segments compared to the expected usage.

4. Case study and results

4.1. Case study and data set

In the United States of America, California exhibits a high level of vulnerability to severe natural disasters, including frequent wildfires and floods (Zigner *et al.* 2022). Santa Barbara County in California is not an exception, as it has faced numerous wildfires throughout its history. Our case study focuses on the Cave Fire in Santa Barbara County to demonstrate how our methodology can be used to assess road network vulnerability to wildfires in a local region. The Cave Fire, a major wildfire that occurred on 25th November 2019, and was contained by 14th December 2019, burned an area of 3126 acres. As the Area of Interest (AoI), the road network of Santa Barbara County obtained from the OSMnx Python package (Boeing 2017), is depicted in Figure 2. The blue lines in this figure illustrate the road network within the AoI, and the red polygon highlights the Cave wildfire perimeter. In this study, we only preserved major road

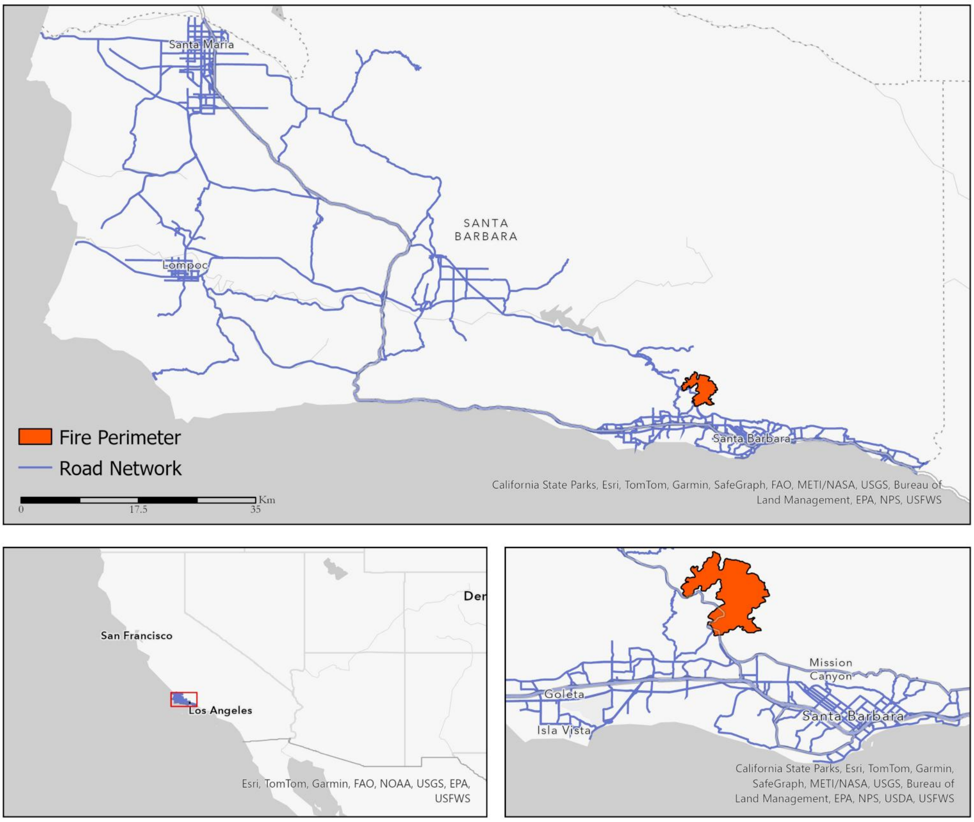

Figure 2. The study area including the road network of Santa Barbara County (upper map), and the city of Santa Barbara (lower right) in California, USA.

segments, including *'Motorway', 'Trunk', 'Primary', 'Secondary', and 'Tertiary'*. These road types can fully capture the spatial configuration and connectivity between Santa Barbara, Lompoc, and Santa Maria cities. Minor road types (e.g. Residential) are excluded as they add to the network's complexity without contributing much in capturing the connectivity between the targeted cities. The full descriptions of these road types can be found in OpenStreetMap (2024a).

Aggregated Location Based Service data is provided by Cuebiq (Cuebiq 2024), a location intelligence platform. Data is collected from anonymized users who have opted-in to provide access to their location data anonymously, through a CCPA and GDPR-compliant framework. The data set used in this study covers the geographical area of Santa Barbara County, starting from 1st November to 30th November 2019. This data set contains 1,184,318 trajectories, with an average temporal resolution of 2 min, and an average accuracy of 10 m.

4.2. Data pre-processing and map matching

We applied map matching on the GPS traces to extract and aggregate daily trajectories on the Santa Barbara road network during the study period. Our initial trajectory

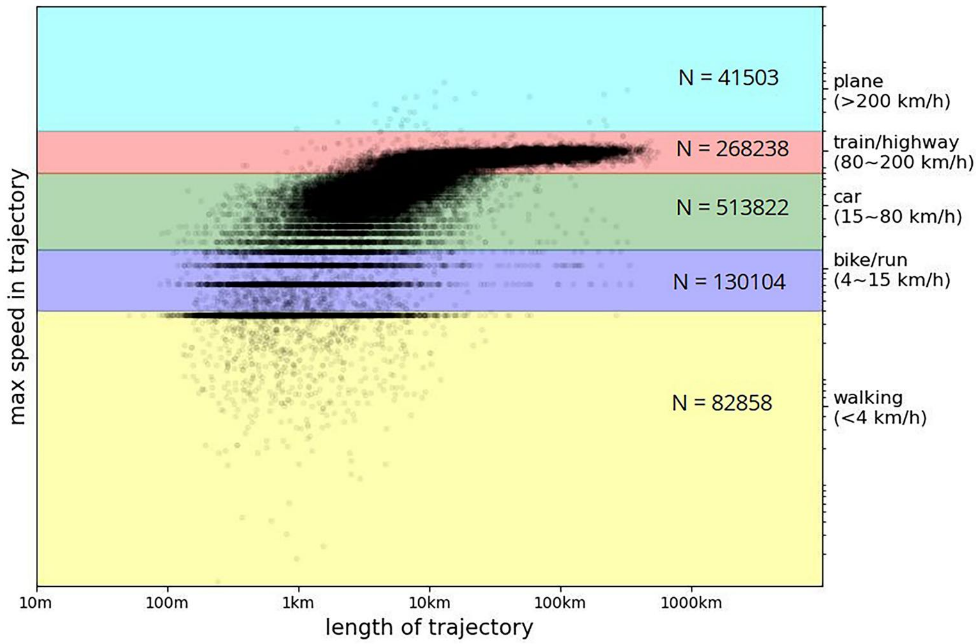

Figure 3. Modes of transportation included in the underlying trajectory data set.

data set contains trajectories from various modes of transportation, including walking, biking, driving, or flying. We applied a simple filtering based on *speed* to distinguish between different modes. In this regard, a given trajectory with speed <4 km/h, between 4 and 15 km/h, 15 and 80 km/h, and 80 and 200 km/h is classified as walking, biking/running, car trip, and train or highway trip, respectively. As depicted in Figure 3, most trajectories pertain to vehicular movement (car, train/highway, and plane). The number of trajectories associated with each mode of transportation is also provided in Figure 3.

The focus of this study is on vehicular movement on roads. That is, only vehicular trajectories that satisfy the conditions $15km/h \leq speed \leq 200km/h$, and $100m \leq length \leq 200km$ are preserved. Implementing the length constraint allows us to filter out outliers and obtain high-quality trajectories. The distribution of the trip lengths and durations are represented in Figures 4(a,b), respectively. Table 1 presents a summary of trajectory counts at each stage of filtering process.

4.3. Variation in movement activity

Figures 5 and 6 demonstrate the movement activity variation based on trajectory count and speed on Monday and Tuesday in the week before the wildfire (18th and 19th November), and Monday and Tuesday when the fire was active (25th and 26th November), and the day after the fire.

A closer look at the movement activity variations reveals that several road segments, in particular parts of the highway HW 154, that are closer to the location of the wildfire exhibited significant movement variations in terms of both trajectory

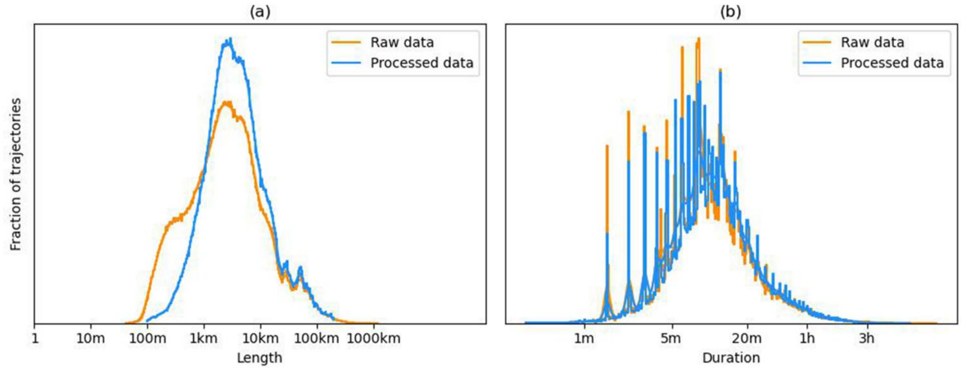

Figure 4. Distributions of the trajectory lengths and durations in the raw and processed data sets.

Table 1. An overview of trajectory counts after each data processing stage.

Processing stage	Initial stage	Trajectory $\succ$ 2 points	15 km/h $\leq$ speed $\leq$ 200 km/h	100 m $\leq$ length $\leq$ 200 km
Number of trajectories	1,184,318	1,036,525	782,060	779,977

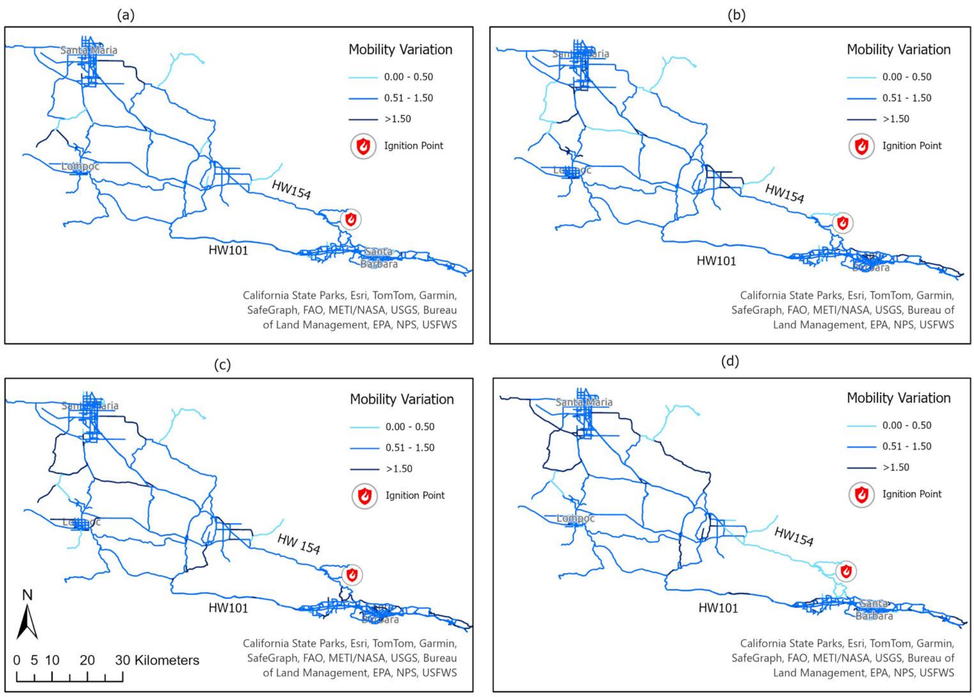

Figure 5. Mobility variation based on trajectory counts on (a) Monday, 18 November 2019, (b) Tuesday, 19 November 2019, (c) Monday, 25 November 2019, and (d) Tuesday, 26 November 2019. The Cave Fire occurred on the evening of November 25.

count and speed compared to the baseline. For example, Figure 5(d) illustrates that the trajectory counts had a significant drop one day after the wildfire. Specifically, HW 154 exhibits a variation of <0.5, meaning that the number of trajectories has

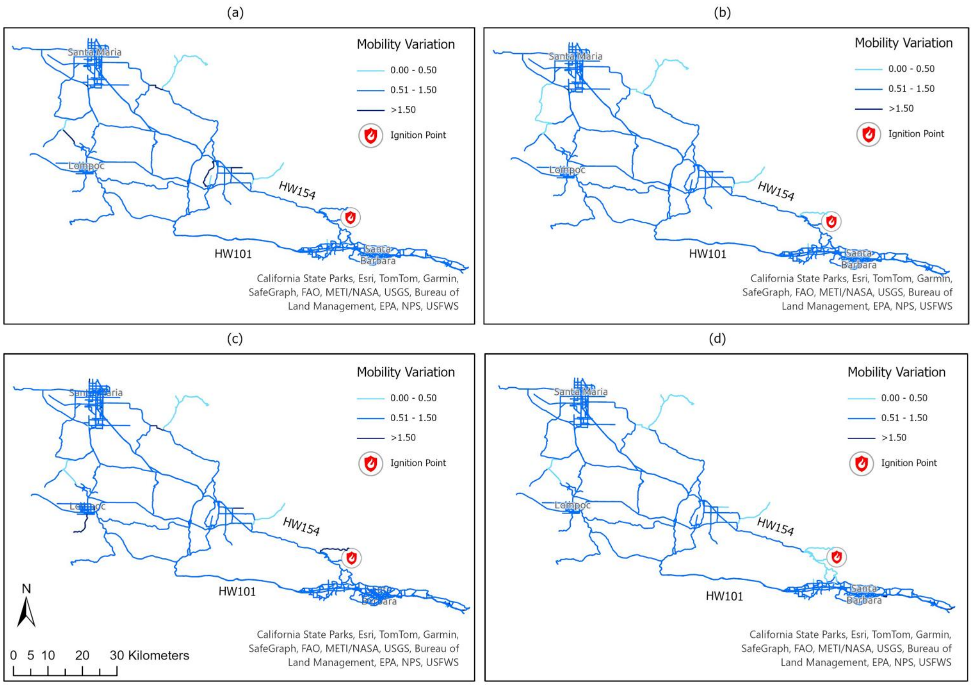

Figure 6. Mobility Variation based on speed on (a) Monday, 18 November 2019, (b) Tuesday, 19 November 2019, (c) Monday, 25 November 2019, and (d) Tuesday, 26 November 2019. The Cave Fire occurred on the evening of 25 November.

significantly decreased compared to the baseline. Figure 6(d) also implies a substantial decrease in trajectory speed for HW 154, with certain areas closer to the wildfire's location displaying a variance of <0.5. This highlights a significant decline in trajectory speeds compared to the baseline.

4.4. Vulnerability assessment

Figure 7 illustrates *BC* values, as an indicator of vulnerability, on each road segment without considering any impact. As it can be seen in the figure, road segments that connect Santa Barbara to Santa Ynez, and also Santa Ynez to Santa Maria are highly vulnerable against disruptions. That is, if these road segments become disabled, the movement flows on the network are greatly impacted.

Considering Figures 5(d) and 7, it appears that Highway 154 became disabled during the Cave Fire. This section of the highway has also high BC value and is identified as a highly vulnerable road segment in the static network.

The road closure identification process, presented in Section 3.3.1, is then performed on daily trajectory data throughout our study period, from 1st November to 30th November 2019. We discovered major road closures (highlighted in red in Figure 8) only on the day following the Cave Fire on November 26. This might be due to the fact the Cave Fire occurred in the evening, and therefore mitigation efforts were carried out on the subsequent day. In Figure 8, the non-functional and functional road segments are indicated with red and gray lines, respectively. As it can be inferred

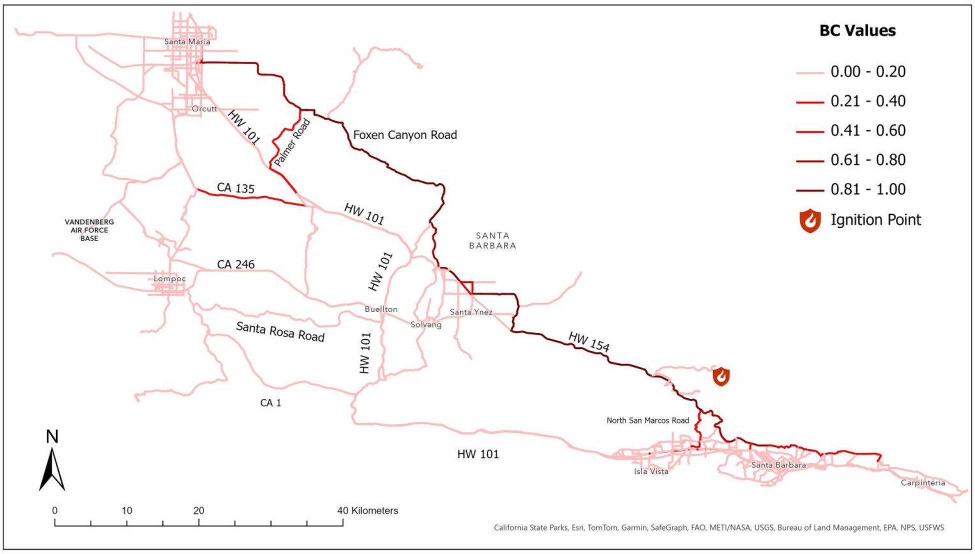

Figure 7. Betweenness centrality (BC) values over the static network, representing the vulnerability of the static network.

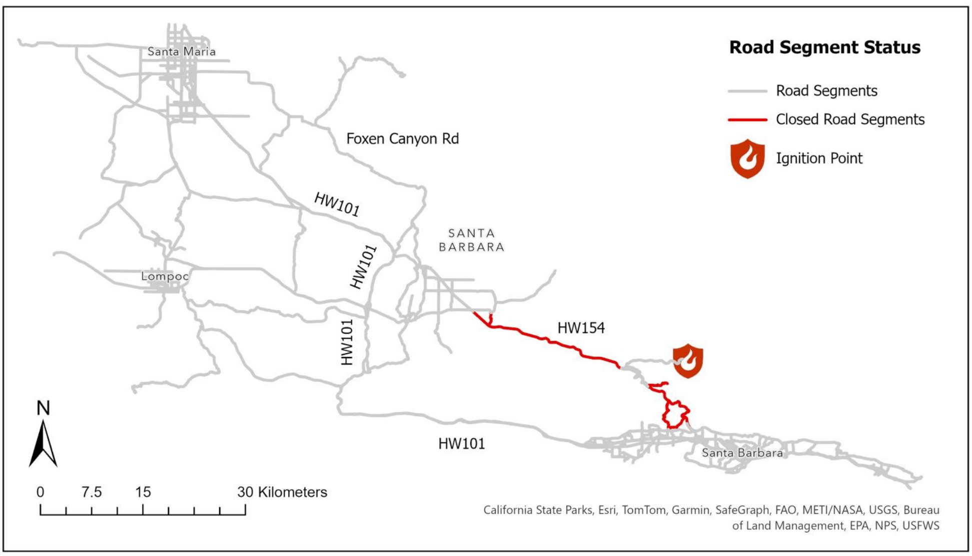

Figure 8. Road closures detected on 26 November 2019.

from this figure, one primary highway (e.g. HW 154), and several tertiary roads became disabled on November 26 as a result of the Cave Fire.

Figure 9 illustrates the BC values over the impacted network on 26 November 2019. The *BC* values over the impacted network are different compared to the static network, highlighting the impact of the Cave Fire on the road network vulnerability. For instance, the *BC* values for several road segments, such as HW CA 1, Foxen Canyon Road, Alisal Road, Ballard Canynon Road, Harris Grade Road, and a part of HW 101

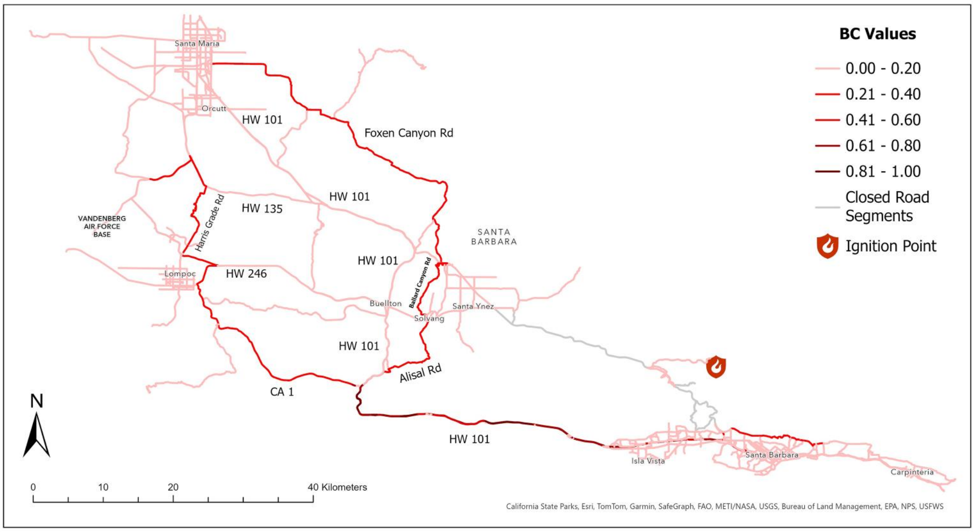

Figure 9. Betweenness centrality (BC) values over the impacted network on 26 November 2019, representing the vulnerability of the static network after the impact.

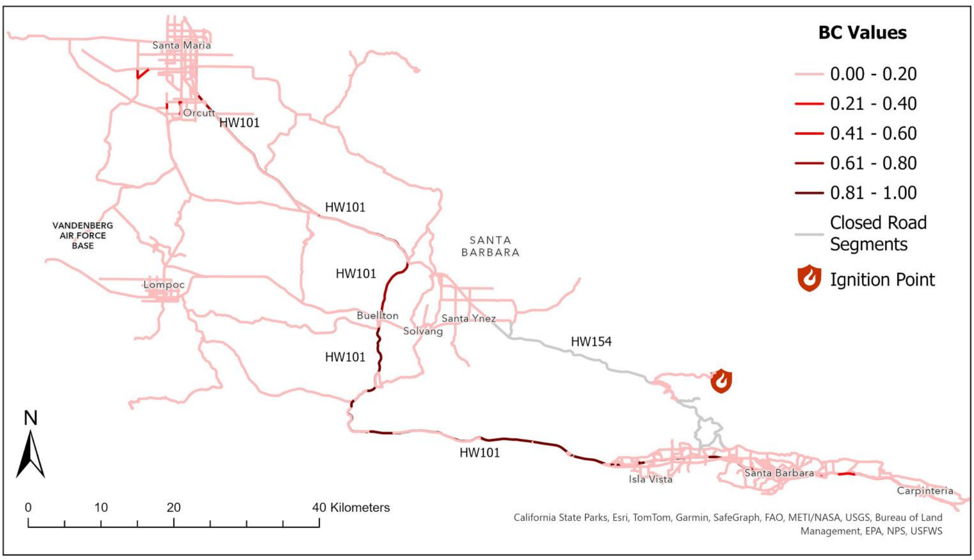

Figure 10. Betweenness centrality (BC) values over the dynamic network on 26 November 2019, representing the vulnerability of the dynamic network after the impact.

exhibit an increase compared to their corresponding values in the static network. This implies that when one or several road segments with high BC values become non-functional within a network, they can impact the entire network.

Figure 10, visualizes the *BC* values over the dynamic network on 26 November 2019, by considering the actual usage of the network as captured in the movement data. This figure reveals a shift in vulnerability values obtained from the dynamic network compared to those from impacted network. The darker a road segment is, the

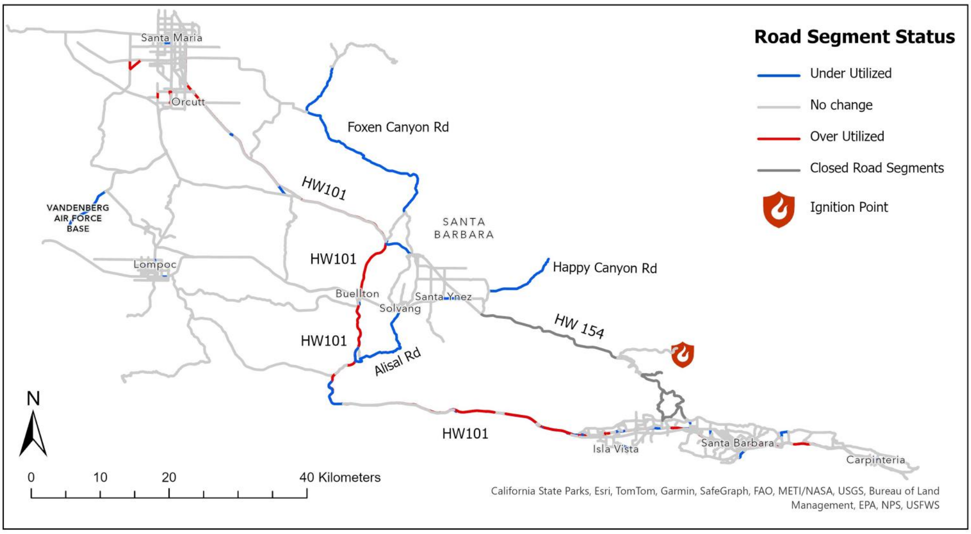

Figure 11. The difference map between static and dynamic vulnerability on 26 November 2019.

higher vulnerability. As illustrated, certain parts of HW 101 exhibit high vulnerability across the dynamic network, while they are not identified as highly vulnerable within the impacted network (see Figure 9).

The *BC* values obtained from the impacted road network offer the vulnerability of the static network after the impact, indicating our anticipation of the vulnerability of the road segments after the removal of certain segments. Conversely, the BC values from the dynamic network present the vulnerability of the dynamic network, reflecting the actual movement activity observed over the network. To further investigate the extent to which the vulnerability values of the dynamic network vary from those in the static network, a difference map is created (Figure 11). In this figure, segments in red represent the over-utilized roads where the value of vulnerability in the dynamic network is greater than those from the static network. That is, these road segments are considered even more susceptible against disruptions when movement activity is taken into account compared to when the vulnerability is estimated only using network topology. Major road segments such as, certain parts of HW 101 are detected as the road segments with increased levels of vulnerability when movement data is included. The road segments in blue, on the other hand, indicate the under-utilized road segments roads in which the value of the vulnerability in the dynamic network is less than those from the static network. Several tertiary road segments including Alisal Road, Foxen Canyon Road, and Happy Canyon Road are the road segments with a decreased level of vulnerability when movement data is involved. Lastly, the road segments in light gray are the roads with no change in vulnerability values when movement activity data is incorporated.

To explore the relationship between road vulnerability and the type of road, Figure 12 classifies the road segments based on their types and vulnerability. The most prominent roads in the U.S. system include, 'Motorway', 'Trunk', 'Primary', 'Secondary', and 'Tertiary', respectively (OpenStreetMap 2024b). 'Trunk' roads are major highways that connect large cities. However, they don't meet the performance requirements to be

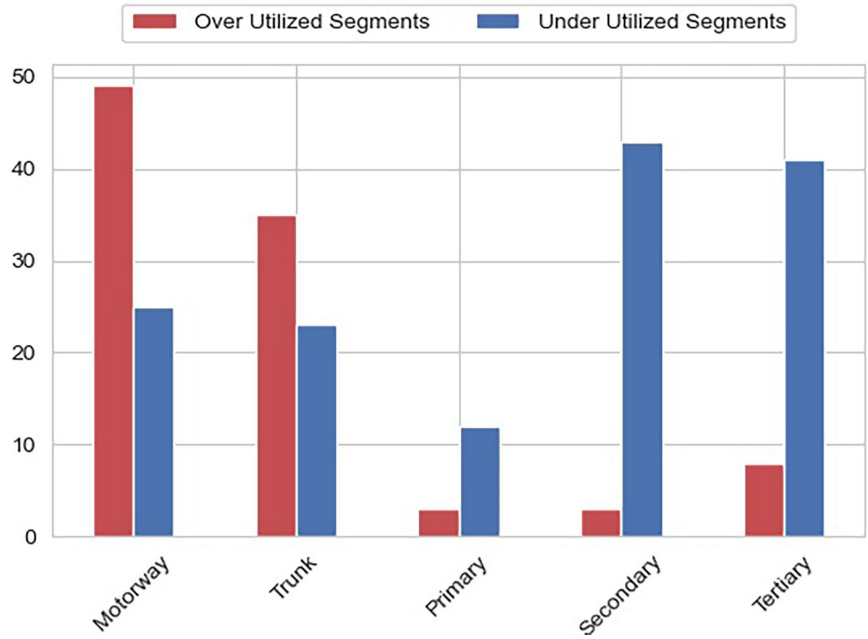

Figure 12. The road network vulnerability classification based on road type.

classified as 'Motorway' or 'Primary'. As seen in Figure 12, major roads, such as *'Motorway'* and *'Trunk'* road segments mainly experience an increased level of centrality when movement activity is considered. Conversely, minor roads, including *'Primary', 'Secondary', and 'Tertiary'* exhibit a decrease in centrality values. That is, incorporating movement activity data shows an over-utilization of major roads and hence an increased level of vulnerability for these roads as compared to minor roads when a disruption occurs. Since our dynamic vulnerability index is a function of individuals' movement during disruptions, this may indicate that during disruptions people tend to use major roads more than minor roads, even if the minor roads may offer shorter routes compared to the major roads.

5. Discussion

To assess the road network vulnerability before, during, and after a disruption, this paper integrates movement data into the static road network to construct a dynamic network. The dynamic road network offers a distinct advantage, as it contains information not only on the spatial structure of the network but also the experienced movement activity over the road network, which in turn, results in an improvement in the estimation of the road network vulnerability in the event of a disruption. Additionally, most existing studies, mainly compare network topology metrics before, during, and after a disruption to evaluate the road network vulnerability. In these approaches, to obtain the impacted network, nodes (e.g. intersections) or links (e.g. road segments) are randomly or intentionally removed, as there is no information or evidence regarding their functionality. However, in this work, the non-functional nodes/links are identified using real movement data. Consequently, the computed impacted network is a more holistic estimation of the road network vulnerability during an actual disruption. The results obtained from this study suggest a shift in the road vulnerability values during the disruption. That is, certain types of road segments become disabled due to the disruption. Our results also indicate that the vulnerability of the road segments changes when integrating movement patterns into the network topology-based models. This can provide insights into how road networks function in reality given a disruption. Identifying the vulnerable road segments within a road network and also understanding how this vulnerability may change during a disruption helps city planners to fortify the vulnerable road segments and also effectively allocate resources during disruptions, ultimately leading to an increase in urban resiliency.

There are several limitations in this study. First, although map matching is not a central focus of this study, the results may still be influenced by the chosen map matching approach. It is also important to note that there is no prefect model for map matching. It is, therefore, a critical need to further study map matching models and improve the current methods. Second, although the representativeness of Cuebiq data used in this study has been investigated in several studies (Wang *et al.* 2019, Aleta *et al.* 2020, Nande *et al.* 2021) with favorable outcomes, the mobile phone data may still not fully capture the true traffic patterns across the road network. One possible solution for this could be integrating movement data from other sources (e.g. Mapbox, Safegraph, and StreetLight), or in-situ traffic sensors to inform the analysis. Additionally, the proposed methodology assumes that mobile tracking data sets are available. However, in areas where mobile phone data access is limited or costly, alternative geospatial datasets that can serve as proxies for individual movement patterns may be used. For example, we can use publicly available traffic census count data, such as Traffic Volumes and Vehicle Miles Traveled (VMT) from state agencies, such as California Department of Transportation (Caltrans 2024). Third, the impacts of disruption on the road network vulnerability depend on both the location, duration, and magnitude of the disruption. Consequently, variations in disruption location and magnitude can lead to differing outcomes on the road network vulnerability. Simulation-based models can play a crucial role in assessing road network vulnerability under various scenarios. For instance, by selectively removing different nodes, they can simulate various disruption locations, and by altering the number of nodes/links removed, they can account for differing disruption magnitudes. However, these approaches are computationally expensive for complex networks. Thus, it becomes crucial to develop models capable of evaluating the vulnerability of complex road networks while considering both the location and magnitude of disruptions. Forth, the selected scale of the study can also influence its outcomes. For instance, the effects of a disruption might be substantial when examining the road network within a Census Block Group (CBG), whereas they may not be noticeable when analyzing the road network within a county. Thus, future research should consider developing models that are less sensitive to the scale of the study. Fifth, as shown in Boeing and Ha (2024), there is a relationship between network design and network vulnerability. That is, some networks are more vulnerable compared to others due to their spatial configuration. Therefore, findings from this study focused on the spatial road network of Santa Barbara, may not be universally applicable to other urban networks with distinct spatial configurations. However, using any road network, the methodology can identify the most vulnerable road segments across the network considering both topology and flow of traffic. Incorporating movement data into betweenness centrality assessment helps identify the road segments that may be critical for network connectivity during disruptions. These segments may not appear vulnerable when assessed solely based on network topology. Our approach captures traffic flow in vulnerability assessment, revealing, for example, segments that might have lower betweenness centrality values but become crucial in network connectivity when real-world traffic patterns are considered. These segments may need spatial attention in evacuation planning or resource allocation. Sixth, identifying vulnerable road segments using only betweenness index in areas with many interconnected roads (e.g. city centers) might be challenging. In such areas, many roads might exhibit high betweenness values, complicating the identification of the most vulnerable road segment. To address this, incorporating other topology indices, such as node degree, clustering coefficient, and closeness can help in accurately identifying the most vulnerable road segments. Lastly, as mentioned in Section 2, previous studies mainly quantify network vulnerability by measuring changes in either network topology or network accessibility indices. While topology-based approaches assess the impacts of disruptions on the network's spatial configuration, accessibility-based models evaluate the impacts of disruptions on individuals' ability to traverse the network and reach important facilities (e.g. hospitals, grocery stores, and shelters). Therefore, current network vulnerability approaches can be strengthened by combining both topology-based and accessibility-based measures. This combination allows for a more holistic understanding of how disruptions affect both the network structure and individuals' satisfactions.

6. Conclusion

This study demonstrates the importance of integrating movement data into static road networks for assessing road network vulnerability. Our findings indicate a shift in the vulnerability values derived from the dynamic network (e.g. when movement activity data is involved) compared to those from the static network. This emphasizes the significance of incorporating movement data into the assessment of the road network vulnerability. Additionally, our results suggest that, in face of disruptive events, individuals tend to use major roads rather than minor roads, even if the minor roads offer shorter routes. This may be due to the faster travel speeds on major roads, allowing people to choose routes that minimize travel time rather than distance. As future research, it would be useful to integrate topology metrics and accessibility indices into a comprehensive vulnerability index, providing a more holistic understanding of road network vulnerability. Moreover, it is important to investigate the impact of scale on the outcomes of the road network vulnerability. The results obtained from this study increase our understanding of how the road network vulnerability may change during disruptions. It can also be useful for city officials to fortify the vulnerable road segments before disruptions, and effectively allocate resources during disruptions, which in turn, leads to an overall improvement in city resilience.

Acknowledgments

Dodge would like to express sincere gratitude to the University of Zurich and ETH Collegium Helveticum program for their support during her sabbatical, which enabled her to focus on writing this research paper.

Disclosure statement

No potential conflict of interest was reported by the author(s).

Funding

The authors gratefully acknowledge the financial support from the U.S. National Science Foundation through award # BCS-2043202.

Notes on contributors

Danial Alizadeh is a PhD student at the Department of Geography at the University of California, Santa Barbara. His research focuses on developing models to measure the impacts of disruptive events on individuals' movement patterns. He contributed to the conceptualization of the methodology, data analysis, code development, and the writing and revising of the paper.

Somayeh Dodge is an associate professor of Spatial Data Science at the Department of Geography at the University of California, Santa Barbara. Her research involves developing spatio-temporal data analytics, machine learning, modeling, and visualization techniques to study and understand movement in human and ecological systems. She contributed to the conceptualization of the methodology, the writing and revision of the paper, and secured funding for the project.

ORCID

Danial Alizadeh http://orcid.org/0009-0000-9459-3078
Somayeh Dodge http://orcid.org/0000-0003-0335-3576

Data and codes availability statement

The data and codes that support the findings of this study can be found using this link.

References

Ahmadzai, F., Rao, K.L., and Ulfat, S., 2019. Assessment and modelling of urban road networks using integrated graph of natural road network (a GIS-based approach). *Journal of Urban Management*, 8 (1), 109–125.

Albert, R., Jeong, H., and Barabasi, A.L., 2000. Error and attack tolerance of complex networks. *Nature*, 406 (6794), 378–382.

Aleta, A., *et al.*, 2020. Modelling the impact of testing, contact tracing and household quarantine on second waves of COVID-19. *Nature Human Behaviour*, 4 (9), 964–971.

Boeing, G., 2016. R-tree spatial index in python. Available from: https://geoffboeing.com/2016/10/r-tree-spatial-index-python/ [Accessed 10 Aug 2023].

Boeing, G., 2017. Osmnx: new methods for acquiring, constructing, analyzing, and visualizing complex street networks. *Computers, Environment and Urban Systems*, 65, 126–139.

Boeing, G. and Ha, J., 2024. Resilient by design: Simulating street network disruptions across every urban area in the world. *Transportation Research Part A: policy and Practice*, 182, 104016.

Brandes, U., 2001. A faster algorithm for betweenness centrality. *The Journal of Mathematical Sociology*, 25 (2), 163–177.

Brandes, U., 2008. On variants of shortest-path betweenness centrality and their generic computation. *Social Networks*, 30 (2), 136–145.

Caltrans, 2024. California Department of Transportation (Caltrans). Available from: https://dot.ca.gov/programs/traffic-operations/census/traffic-volumes [Accessed 12 Sep 2024].

Chao, P., *et al.*, 2020. A survey on map-matching algorithms. *In*: *Databases Theory and Applications: 31st Australasian Database Conference, ADC 2020, Proceedings 31*, Melbourne, VIC, Australia, 3–7 February 2020. Springer, 121–133.

Church, R.L., Scaparra, M.P., and Middleton, R.S., 2004. Identifying critical infrastructure: the median and covering facility interdiction problems. *Annals of the Association of American Geographers*, 94 (3), 491–502.

Cuebiq, 2024. Cuebiq company. Available from: https://www.cuebiq.com/ [Accessed 16 Jan 2024].

Demšar, U., Špatenková, O., and Virrantaus, K., 2008. Identifying critical locations in a spatial network with graph theory. *Transactions in GIS*, 12 (1), 61–82.

Feng, J., *et al.*, 2020. Deepmm: deep learning based map matching with data augmentation. *IEEE Transactions on Mobile Computing*, 21, 1–1.

Fraser, A.M., Chester, M.V., and Underwood, B.S., 2022. Wildfire risk, post-fire debris flows, and transportation infrastructure vulnerability. *Sustainable and Resilient Infrastructure*, 7 (3), 188–200.

Freeman, L.C., *et al.*, 2002. Centrality in social networks: conceptual clarification. *In*: *Social network: critical concepts in sociology*. London: Routledge, vol. 1, 238–263.

Furno, A., *et al.*, 2021. Graph-based ahead monitoring of vulnerabilities in large dynamic transportation networks. *PLOS One*, 16 (3), e0248764.

Gu, Y., Chen, A., and Kitthamkesorn, S., 2022. Accessibility-based vulnerability analysis of multimodal transportation networks with weibit choice models. *Multimodal Transportation*, 1 (3), 100029.

Hagberg, A., Swart, P., and Chult, D.S., 2008. *Exploring network structure, dynamics, and function using NetworkX*. Technical Report. Los Alamos, NM: Los Alamos National Lab (LANL).

Hu, Y. and Lu, B., 2019. A hidden Markov model-based map matching algorithm for low sampling rate trajectory data. *IEEE Access*, 7, 178235–178245.

Huang, Z. and Loo, B.P., 2023. Vulnerability assessment of urban rail transit in face of disruptions: a framework and some lessons from Hong Kong. *Sustainable Cities and Society*, 98, 104858.

Jayasinghe, A., *et al.*, 2019. A novel approach to model traffic on road segments of large-scale urban road networks. *MethodsX*, 6, 1147–1163.

Matisziw, T.C. and Murray, A.T., 2009. Modeling s–t path availability to support disaster vulnerability assessment of network infrastructure. *Computers & Operations Research*, 36 (1), 16–26.

Matisziw, T.C., Murray, A.T., and Grubesic, T.H., 2009. Exploring the vulnerability of network infrastructure to disruption. *The Annals of Regional Science*, 43 (2), 307–321.

Mattsson, L.G. and Jenelius, E., 2015. Vulnerability and resilience of transport systems–a discussion of recent research. *Transportation Research Part A: Policy and Practice*, 81, 16–34.

Moore, D.S. and McCabe, G.P., 1989. *Introduction to the practice of statistics*. New York: WH Freeman/Times Books/Henry Holt & Co.

Murray, A.T., Matisziw, T.C., and Grubesic, T.H., 2008. A methodological overview of network vulnerability analysis. *Growth and Change*, 39 (4), 573–592.

Nande, A., *et al.*, 2021. The effect of eviction moratoria on the transmission of SARS-CoV-2. *Nature Communications*, 12 (1), 2274.

OpenStreetMap, 2024a. Road classification based on wiki open street map. Available from: https://wiki.openstreetmap.org/wiki/United_States/Road_classification [Accessed 16 Jan 2024].

OpenStreetMap, 2024b. Road classification based on wiki open street map. Available from: https://wiki.openstreetmap.org/wiki/Key:highway [Accessed 16 Jan 2024].

Papilloud, T. and Keiler, M., 2021. Vulnerability patterns of road network to extreme floods based on accessibility measures. *Transportation Research Part D: Transport and Environment*, 100, 103045.

Quddus, M.A., Ochieng, W.Y., and Noland, R.B., 2007. Current map-matching algorithms for transport applications: state-of-the art and future research directions. *Transportation Research Part C: Emerging Technologies*, 15 (5), 312–328.

Shi, J., *et al.*, 2019. Sustainable development of urban rail transit networks: a vulnerability perspective. *Sustainability*, 11 (5), 1335.

Suarez, P., *et al.*, 2005. Impacts of flooding and climate change on urban transportation: a systemwide performance assessment of the Boston metro area. *Transportation Research Part D: Transport and Environment*, 10 (3), 231–244.

Sun, D., Zhao, Y., and Lu, Q.C., 2015. Vulnerability analysis of urban rail transit networks: a case study of Shanghai, China. *Sustainability*, 7 (6), 6919–6936.

Sun, L., *et al.*, 2018. Vulnerability assessment of urban rail transit based on multi-static weighted method in Beijing, China. *Transportation Research Part A: Policy and Practice*, 108, 12–24.

Taylor, M.A., 2008. Critical transport infrastructure in urban areas: impacts of traffic incidents assessed using accessibility-based network vulnerability analysis. *Growth and Change*, 39 (4), 593–616.

Testa, A.C., Furtado, M.N., and Alipour, A., 2015. Resilience of coastal transportation networks faced with extreme climatic events. *Transportation Research Record: Journal of the Transportation Research Board*, 2532 (1), 29–36.

Tukey, J.W., *et al.*, 1977. *Exploratory data analysis*. Vol. 2. Reading, MA: John W. Tukey.

Wang, F., *et al.*, 2019. Extracting trips from multi-sourced data for mobility pattern analysis: an app-based data example. *Transportation Research. Part C, Emerging Technologies*, 105, 183–202.

Zhang, Y., *et al.*, 2011. Centrality characteristics of road network patterns of traffic analysis zones. *Transportation Research Record: Journal of the Transportation Research Board*, 2256 (1), 16–24.

Zhu, Y., Jiang, M., and Yamamoto, T., 2022. Glocal map-matching algorithm for high-frequency and large-scale GPS data. *Journal of Intelligent Transportation Systems*, 28 (1), 1–15.

Zigner, K., *et al.*, 2022. Wildfire risk in the complex terrain of the Santa Barbara wildland–urban interface during extreme winds. *Fire*, 5 (5), 138.